

Compact Ultrawideband Antenna Backed by an Artificial Magnetic Conductor

Khalid M. Ibrahim, Eman M. Eldesouki*, and Ahmed M. Attiya

Abstract—In this paper, a new artificial magnetic conductor (AMC) structure is proposed to enhance the performance of an ultra-wideband (UWB) antenna for wireless communication networks. A fractal configuration is used to introduce the UWB performance of the proposed antenna. The antenna is composed of a modified rectangular patch antenna with a tapered section fed by a coplanar waveguide (CPW) with a total size of $24 \times 20 \times 1.5 \text{ mm}^3$. The antenna is backed by an AMC. The proposed AMC unit consists of a square patch surrounded by four slotted square rings. This unit cell exhibits an in-phase reflection from 6.3 GHz to 10 GHz. The obtained bandwidth of the antenna with AMC is 110% from 3.2 GHz to 11 GHz which covers the entire UWB range. The peak gain of 7.2 dB is accomplished with a compact size of $40 \times 40 \times 6.5 \text{ mm}^3$, $0.95 \times 0.95 \times 0.15\lambda_0$ at 7.1 GHz. The proposed UWB antenna-AMC is fabricated and measured for verification.

1. INTRODUCTION

Low profile high gain planar antennas are widely used in wireless communication networks, radar imaging, and ground penetrating radar [1]. Planar structures are used to design compact antennas due to their features of light weight, low cost, conformability, and easy fabrication [2]. The improvements of bandwidth and gain for wide band application are required simultaneously for different applications. These can be achieved by adding an electrically conducting reflector below the antenna at a fixed distance of quarter wavelength [3, 4]. This increases the total antenna profile. Moreover, the radiation properties cannot be enhanced over a wide bandwidth. To solve this problem, various techniques have been introduced to improve the radiation properties of the antenna without affecting the impedance bandwidth and return loss. An example for these methods is replacing electrically conducting reflectors by partially reflective surfaces (PRS) [5], frequency selective surfaces (FSS) [6–8], meta-surface [9, 10], and artificial magnetic conductor (AMC) [11–14].

Recently, different geometries of AMC are introduced as reflectors to improve the radiation performance of the wideband antenna with reduced profile [11–20]. For example in [18], an enhancement of 2.3 dB in gain is achieved by placing an AMC reflector below a compact aperture coupled stepped dielectric resonator UWB multiple-input multiple-output (MIMO) antenna. Although the gain in [19] is higher than 8 dB, this antenna occupies large space which limits its application areas. So, it is a challenge task to design a low profile, low cost, and light weight wideband antenna with improved gain and high efficiency.

AMC structures are characterized by equivalent high impedance surface with in-phase reflection property in the range from -90° to $+90^\circ$ [21, 22]. This property makes the reflected wave by AMC in phase with the incident one. This leads to the accumulative superposition of radiation from antenna. By using the AMC structure, the limitation of $\lambda/4$ between the antenna and reflector is not required, and the total antenna size can be reduced.

Received 29 April 2023, Accepted 10 June 2023, Scheduled 19 June 2023

* Corresponding author: Eman M. Eldesouki (eman@eri.sci.eg).

The authors are with the Microwave Engineering Department, Electronics Research Institute (ERI), Cairo, Egypt.

In this paper, a novel UWBCPW monopole antenna backed by a wideband AMC structure is presented to improve the antenna gain without affecting the impedance bandwidth. This property is important for wireless communication networks to reach high data rate bandwidth connections with a low level of power consumption [23, 24]. The proposed UWB antenna is achieved after a series of modifications in conventional rectangular patch antenna in order to expand the operating bandwidth. An enhancement in the antenna gain by 2.5 to 5 dB with directional radiation pattern over a wide impedance band of 3.2–11 GHz is achieved by adding a wideband AMC below the designed antenna. The distance between antenna and AMC is optimized for maximum gain and bandwidth. The proposed antenna-AMC is fabricated by using a low-cost FR-4 material and measured for verification. The designed antenna shows a wide bandwidth, good gain, high efficiency, and compact size.

This paper is organized as follows. Section 2 presents the design steps of the proposed UWB antenna. The design of the AMC is presented in Section 3. Thereafter, Section 4 includes the design of the UWB antenna with AMC. Section 5 presents the simulated and measured results of the UWB antenna-AMC followed by the conclusion in Section 6.

2. DESIGN OF ULTRA-WIDEBAND ANTENNA

Design steps of the proposed UWB antenna are shown in Fig. 1, and the corresponding reflection coefficient for each step is shown in Fig. 2. Four optimization stages are performed to achieve the final design of the antenna. The substrate is FR4 with a dielectric constant ϵ_r of 4.2 and a thickness of 1.5 mm. The total size of the antenna is (24×20) mm². The feeding network is CPW microstrip line with a transmission width of 1.5 mm and a gap of 0.25 mm between the transmission line and the ground plane to obtain 50Ω of impedance.

The design process starts with Antenna 1 which is a rectangular patch antenna of dimensions $17.5 \text{ mm} \times 17 \text{ mm}$ with a linearly tapered section to improve the matching with the feeding line. In this

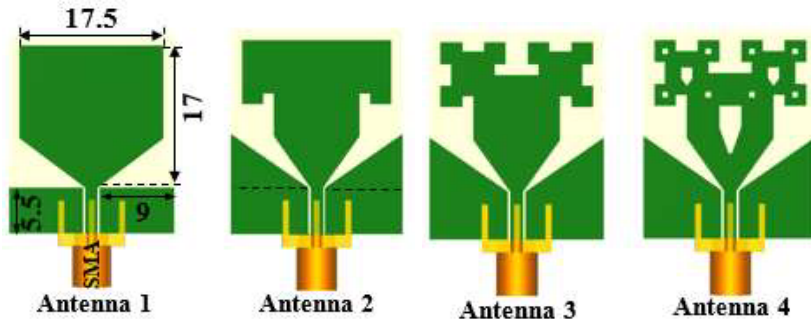


Figure 1. Geometries of the different design steps of the proposed UWB monopole antenna.

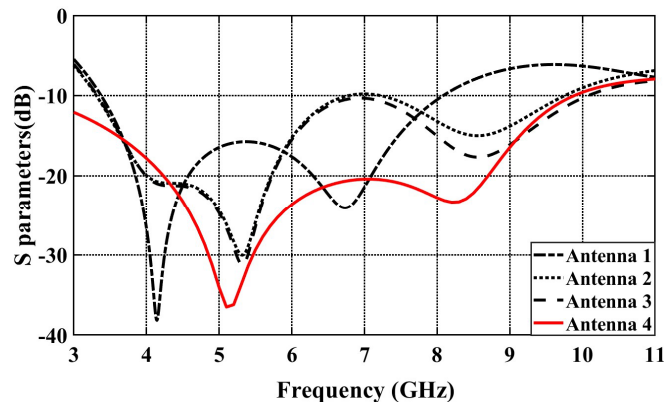


Figure 2. Reflection coefficients for the different design steps of the proposed UWB monopole antenna.

case, the bandwidth of $S_{11} < -10$ dB is from 3.4 to 8 GHz. This bandwidth is improved by changing the upper two corners of the rectangular patch to fractal rectangular patches in two steps. In addition, the ground plane of the CPW is also tapered to improve the bandwidth of the antenna. More improvement of the bandwidth is obtained by subtracting fractal slots of the shape of the original rectangular patch with the tapered section. The bandwidth of Antenna 4 with the fractal rectangular patches and fractal slots is expanded to be 110% in the range from 3 to 11.

The geometry of the optimized UWB antenna is shown in Fig. 3. On the other hand, the equivalent circuit model of the proposed UWB antenna is shown in Fig. 4(a). Foster first canonical circuit is used to represent its equivalent circuit [25]. Two parallel RLC circuits connected in series are used to model the antenna and produce its operating frequency bandwidth. Elements $R_2, L_2,$ and C_2 resonate in the lower frequency band from 3 to 9 GHz. The response of the higher frequency band 9–11 GHz can be produced by adjusting the values of $R_3, L_3,$ and C_3 . Since the UWB is composed of lower and higher frequency bands, two parallel RLC circuits are required to represent this behavior. Discrete elements $R_1, L_1,$ and C_1 are used to model the CPW transition and SMA connector. Numerical simulations of

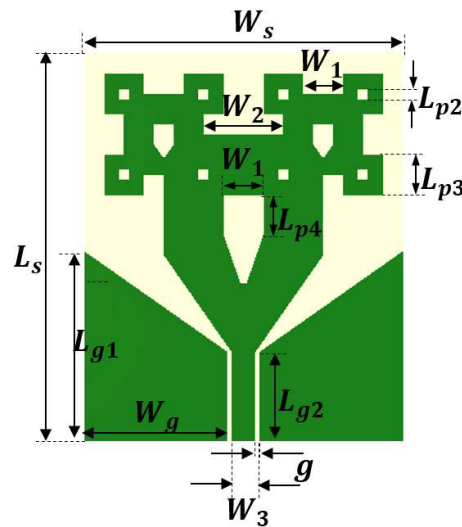


Figure 3. Geometry of the optimized antenna: $W_s = 20, W_g = 9$ mm, $W_1 = 2.5$ mm, $W_2 = 5$ mm, $W_3 = 1.75$ mm, $L_s = 24$ mm, $L_{g1} = 11.75$ mm, $L_{g2} = 5.5$ mm, $L_{p2} = 0.625, L_{p3} = L_{p4} = 2.5$ mm, $g = 0.25$ mm.

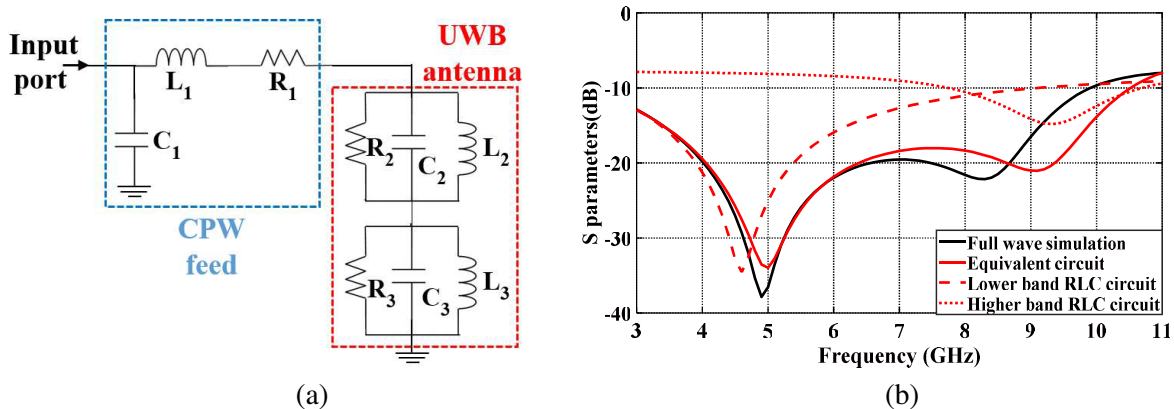


Figure 4. (a) Equivalent circuit model: $R_1 = 21 \Omega, R_2 = 27 \Omega, R_3 = 51 \Omega, L_1 = 0.051$ nH, $L_2 = 0.9$ nH, $L_3 = 0.16$ nH, $C_1 = 0.01$ pF, $C_2 = 1.3$ pF, $C_3 = 1.7$ pF; (b) Reflection coefficients of the full wave analysis and the equivalent network.

the proposed antenna are developed by using CST and ADS. Good agreement between the simulated reflection coefficients is obtained from the full wave electromagnetic (EM) simulator and equivalent circuit model, as shown in Fig. 4(b).

The surface current density on the surface of final design at different frequencies is shown in Fig. 5. It can be noted that high current is concentrated around the lower edges in the lower frequency band. As the frequency increases, the current density on the upper edges increases. This explains the main role of the fractal parts on the upper corner in increasing the operating bandwidth.

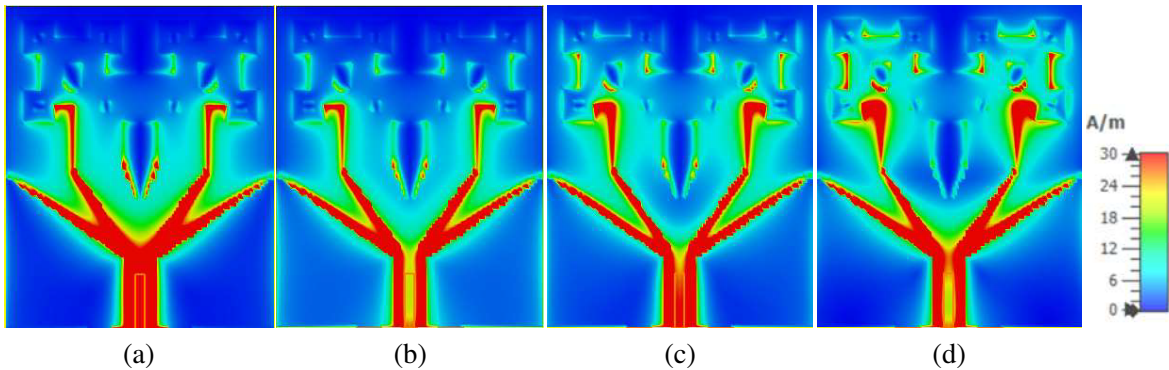


Figure 5. Surface current density on the designed UWB antenna at different frequencies (a) 3 GHz; (b) 5.5 GHz; (c) 7 GHz; (d) 9 GHz.

3. DESIGN OF THE REFLECTING ARTIFICIAL MAGNETIC SURFACE

Ideal artificial magnetic surface is characterized by a unity reflection coefficient with a phase shift equal to zero for the reflected electric field. This can be implemented by using a periodic resonance structure. This resonance performance can be obtained by using periodic patches loaded by via posts on a grounded dielectric slab. The periodic patches introduce the capacitive effect while the via posts introduce the inductive effect. The disadvantage of this method is the complexity in fabrication process due to the via posts. As an alternative configuration, the unit cell of the AMC is composed of a patch which is surrounded by a slotted ring or multi-slotted rings as shown in Fig. 6(a). In this case, these slotted rings introduce the required inductive effect without the need for via posts.

The design of the AMC unit cell starts with (AMC1) which consists of a centered square patch of length 1.6 mm enclosed by one slotted ring of width 1.4 mm on a grounded FR4 substrate of a thickness 3 mm. The outer size of the ring is $4.8 \times 4.8 \text{ mm}^2$ with the spacing distance between each two adjacent

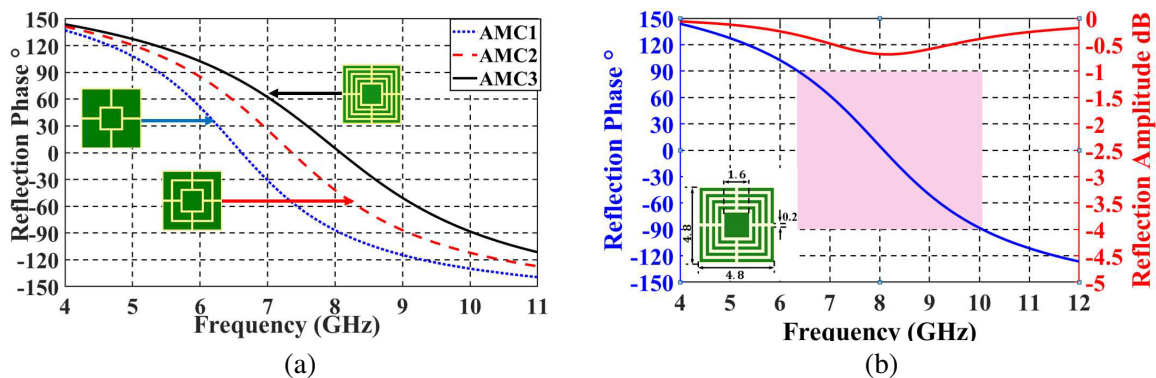


Figure 6. Proposed AMC unit cell. (a) Variation of reflection phases of three AMC structures; (b) Amplitude and phase of the reflection coefficient of the unit cell in periodic boundary conditions.

unit cells equal to 0.2 mm. This unit cell provides a bandwidth of 39% from 5.4 GHz to 8.1 GHz with zero-degree reflection phase at 6.6 GHz. By dividing the outer ring into two concentric rings (AMC2), the in-phase reflection bandwidth is increased to 42% from 5.8 GHz to 9.1 GHz with 0° reflection phase point shifted to 7.4 GHz. By dividing the outer ring into four concentric rings (AMC3), the in-phase reflection bandwidth is increased to be in the frequency range from 6.3 to 10 GHz. In this range, this AMC can be used to enhance the performance of the designed antenna as discussed in the following section. Fig. 6(b) shows the magnitude and phase of the reflection of this AMC. From these results it can be observed that this unit provides a total reflection behavior with reflection phase ranged between -90° and $+90^\circ$ with zero-degree reflection phase point observed about 8.1 GHz.

4. ULTRA-WIDEBAND ANTENNA BACKED BY AMC

The designed UWB antenna proposed in Section 2 is backed by the AMC designed in Section 3 at a distance d from the antennas as depicted in Fig. 7(a). A foam spacer of thickness d is added between the antenna and the AMC surface as shown in Fig. 7(b). To determine the optimal distance between the antenna and the AMC sheet and the optimal number of the used AMC unit cells for the reflector surface, parametric analyses in terms of impedance matching and maximum gain over the operating frequency band are carried out in this section. Moreover, the effect of adding perfect electric conductor (PEC) surface with the same size of AMC reflector at various distances d between reflector surface and UWB antenna is also presented.

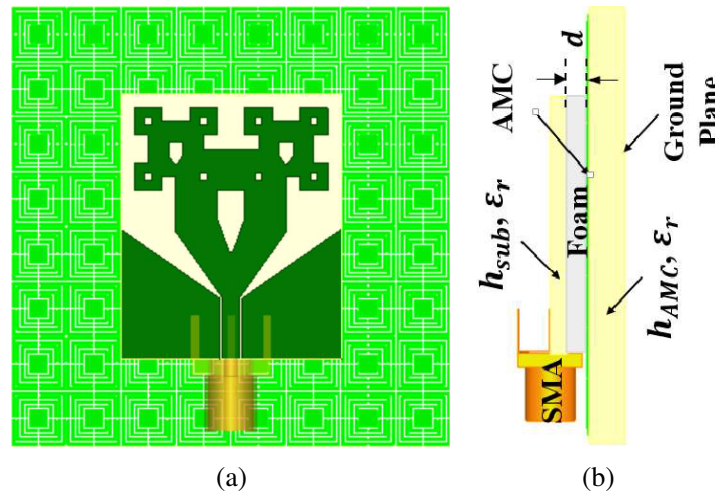


Figure 7. Geometry the proposed UWB antenna backed by the AMC. (a) Top view; (b) Side view.

To study the effect of varying the distance between the antenna and the AMC reflector, an array of 8×8 AMC unit cells with dimensions of $(40 \times 40 \times 3) \text{ mm}^3$ is used as a reflecting plane. The simulated S_{11} for the UWB antenna backed by AMC surface at different distances d is shown in Fig. 8(a). From this figure, it can be noted that by increasing d from 1 mm to 4 mm, a small variation in lower and upper frequency edges of the operating bands is observed. On the other hand, the effect of changing d on the peak gain is shown in Fig. 8(b). It can be noted that the best distance corresponds to $\lambda_o/20$ at the center frequency of 7.1 GHz.

Also, the number of used AMC unit cells limits the overall size and the performance of the antenna. The peak gain is studied for different cases; specifically 6×6 , 8×8 , and 10×10 unit cells with dimensions of $30 \times 30 \times 6.5 \text{ mm}^3$, $40 \times 40 \times 6.5 \text{ mm}^3$, and $50 \times 50 \times 6.5 \text{ mm}^3$, respectively. The variation of the peak gain for different array sizes is shown in Fig. 9. From this figure, it can be noted that a peak gain is nearly saturated for 8×8 unit cells. Thus, the array of 8×8 AMC unit cells is chosen to provide the maximum bandwidth and peak gain with minimum antenna-AMC size of $40 \times 40 \times 6.5 \text{ mm}^3$, $(0.95 \times 0.95 \times 0.15)\lambda_o$.

To prove that the AMC structure can reduce the antenna profile, it is compared with the situation

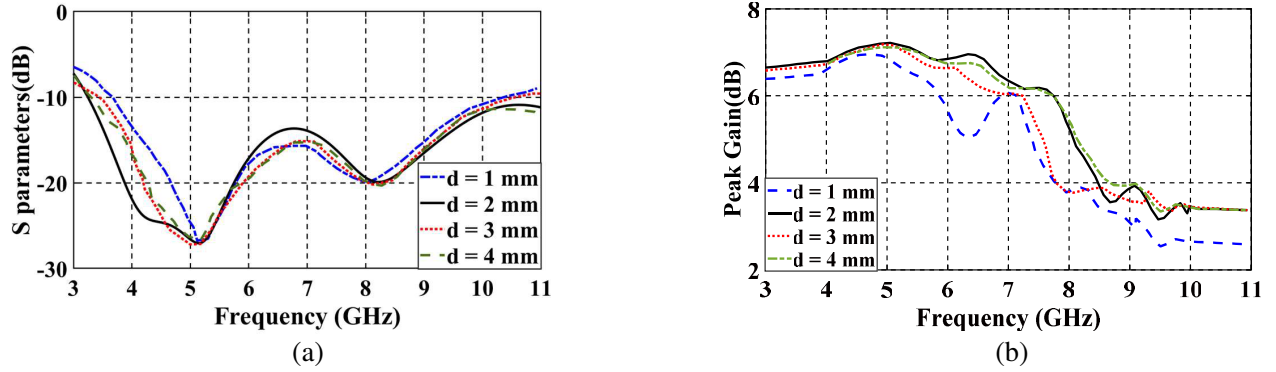


Figure 8. Effect of varying the distance between the antenna and the AMC reflector. (a) Magnitude of reflection coefficient $|S_{11}|$, and (b) frequency response of the peak gain.

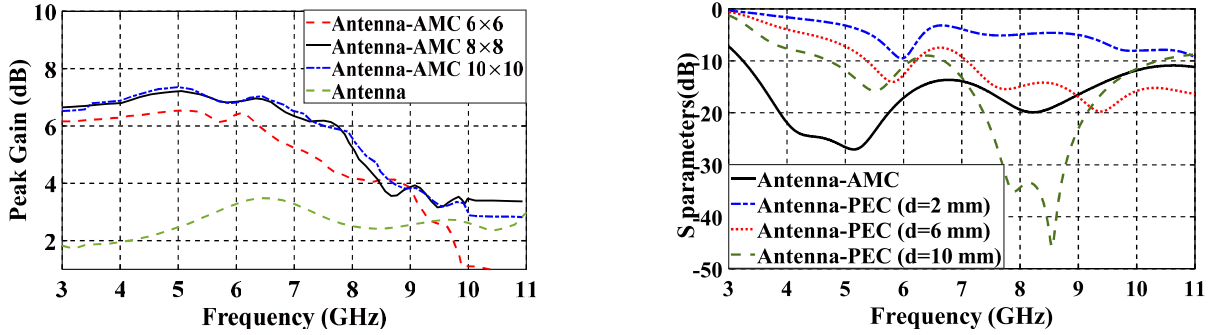


Figure 9. Dependence of the peak gain on the number of the used AMC unit cells.

Figure 10. Reflection coefficients for the proposed UWB antenna with AMC and PEC reflecting plane at different distances.

Table 1. Comparison of the proposed antenna-AMC with some recent works.

Reference	Operating Frequency band (GHz)	Physical Dimensions (mm^3)	Electrical Dimensions (λ_o)	Impedance BW (%)	AMC BW (%)	Peak Gain (dB)	Average peak gain enhanced (dB)
[11]	3.13–8.41	$56 \times 56 \times 16.2$	$1.08 \times 1.08 \times 0.32$	91%	45%	7.9	4.7
[12]	2.7–11.8	$100 \times 100 \times 15$	$2.4 \times 2.4 \times 0.36$	125%	64%	9.5	3.74
[13]	8.2–13	$36 \times 48 \times 6.12$	$1.3 \times 1.7 \times 0.22$	45%	40%	7.04	3.5
[14]	4.77–7.07	$60 \times 60 \times 6$	$1.2 \times 1.2 \times 0.12$	40%	15%	9.9	-
[15]	4.96–5.90	$42 \times 28 \times 4$	$1.78 \times 1.78 \times 0.07$	29%	118%	6.7	1.5
[16]	3–4.1	$75 \times 75 \times 17$	$0.87 \times 0.78 \times 0.19$	31%	30%	7	-
[17]	3.8–10.6	$33 \times 33 \times 21.6$	$0.77 \times 0.77 \times 0.71$	94%	105%	8	3.5
proposed	3.2–11	$40 \times 40 \times 6.5$	$0.95 \times 0.95 \times 0.15$	110%	45%	7.2	5

that the antenna is backed by PEC. The size of the PEC sheet is the same as the AMC sheet. The comparison results of the simulated S_{11} for different values of d are shown in Fig. 10. It can be noted that when the antenna is loaded with PEC placed at $d = 10$ mm, the thickness of the overall antenna is increased to 14.5 mm ($0.34\lambda_o$) to obtain a bandwidth of 43% from 6.7 to 10.53 GHz. For the case $d = 2$ mm, the impedance matching deteriorates, and the bandwidth decreases. On the other hand, replacing the PEC by the proposed AMC structure at a distance of 2 mm, the impedance matching is

improved to 110% from 3.2 GHz to 11 GHz. According to this comparison, it can be concluded that the proposed AMC can significantly improve the operating bandwidth with much lower profile. On the other hand, Table 1 presents other comparisons with existing AMC-based antennas in literature. The results collected in Table 1 indicate that the proposed antenna outperforms the selected structures in terms of average peak gain enhanced. Also, it offers a smaller size than all compared structures.

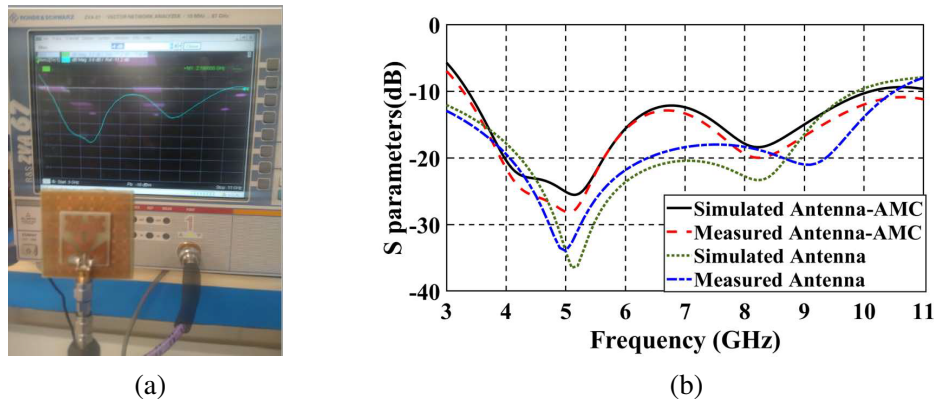


Figure 11. (a) Measurement setup of S -parameter; (b) Simulated and measured $|S_{11}|$ results of the proposed UWB with and without AMC.

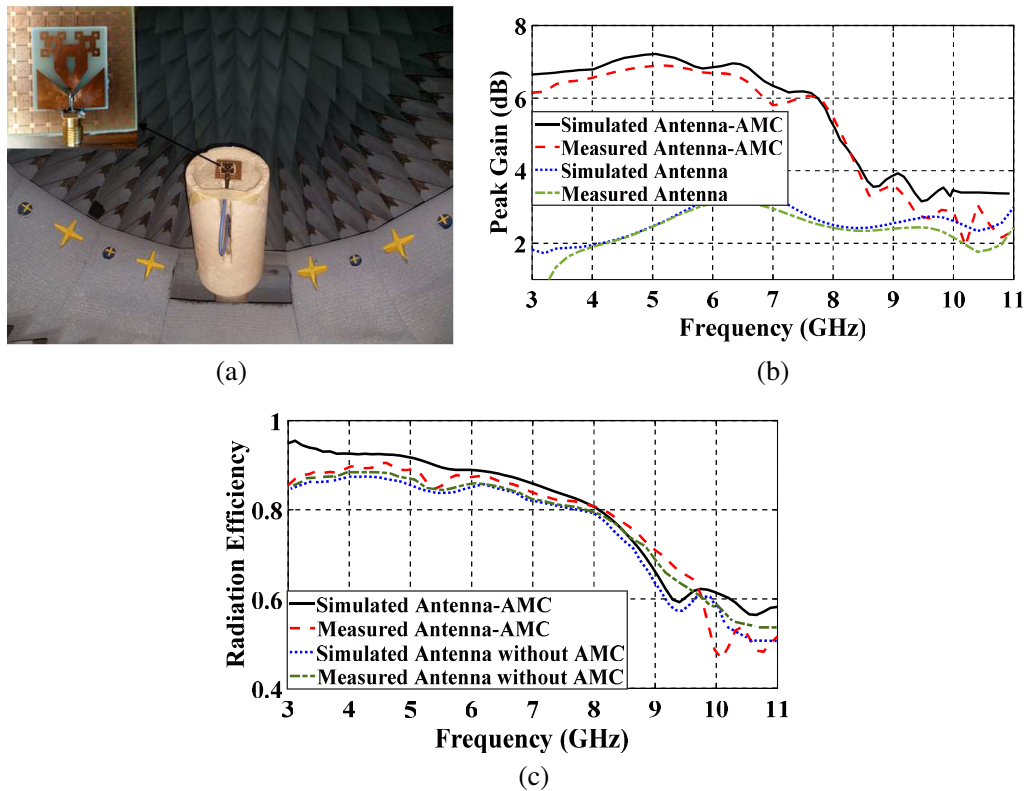


Figure 12. (a) Fabricated model of the UWB antenna-AMC inside the Starlab measurement system, (b) frequency response of the simulated and measured peak gain of the proposed UWB with and without AMC, and (c) frequency response of the simulated and measured radiation efficiency of the proposed UWB with and without AMC.

5. EXPERIMENTAL RESULTS

The designed UWB antenna with an AMC structure is fabricated and measured for verification. A layer of foam with thickness of 2 mm and $\epsilon_r \approx 1.07$ is added to separate between antenna and AMC. The S -parameter of the fabricated antenna-AMC is measured by using Rhode and Schwartz model ZVA67 VNA as shown in Fig. 11(a). Fig. 11(b) shows the simulated and measured $|S_{11}|$ results for the proposed antenna, both with and without the AMC structure. It can be noted that the measured results prove that operating bandwidth ($S_{11} < -10$ dB) is from 3.2 GHz to 11 GHz (110%). A slight deviation in measured results is observed mainly because of fabrication tolerance, assembly errors, imperfect soldering, and measurement environment. The far field measurements have been utilized using the antenna measurement system Starlab 18 as shown in Fig. 12(a). The frequency responses of the measured maximum gain and radiation efficiency are shown in Figs. 12(b) and (c) for the proposed

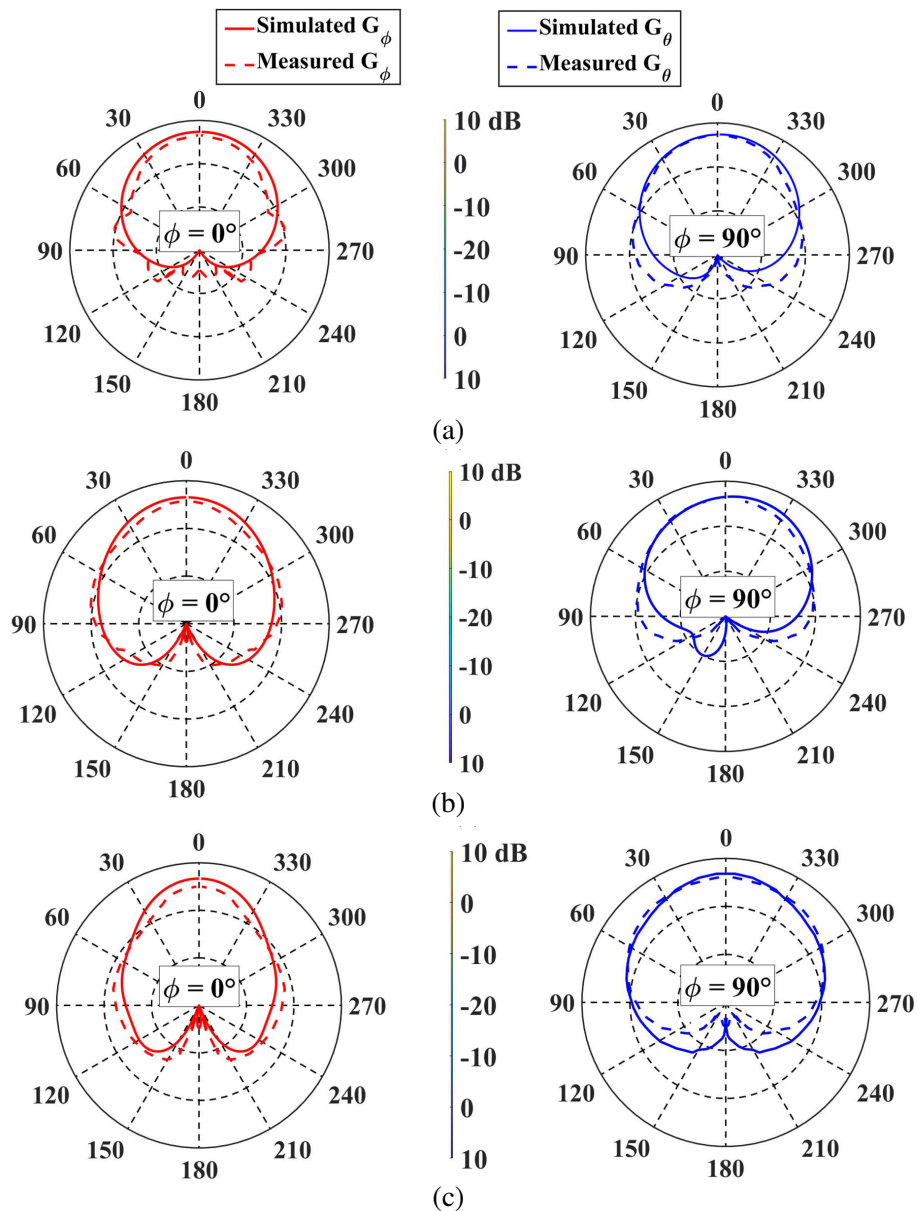


Figure 13. Radiation patterns at (a) 5.5 GHz; (b) Radiation patterns at 7 GHz; (c) Radiation patterns at 8 GHz.

antenna with and without AMC. The measured gain is around 7 dB within the operating band 4–7.8 GHz with enhancement of 1.5 to 4.5 dB achieved by adding AMC. The measured efficiency is over 70% within the working bandwidth 4–8.8 GHz with good agreement between the simulated and measured values. The simulated and measured radiation patterns in two planes $\phi = 0^\circ$ and $\phi = 90^\circ$ at 5.5, 7, and 8 GHz are shown in Fig. 13. It can be noted that good unidirectional radiation patterns with lower side lobe levels are obtained.

6. CONCLUSION

In this paper, a new UWB antenna based on a rectangular patch with tapered feeding and loaded by fractal corners is introduced for wireless communication networks. The proposed UWB antenna is achieved after a series of modifications in conventional rectangular patch antenna in order to expand the operating bandwidth. By adding an AMC reflecting surface behind the antenna, the gain is improved without affecting the impedance bandwidth. The proposed AMC unit cell is composed of a square patch surrounded by four slotted square rings. This AMC introduces in phase reflection over a bandwidth of 45% from 6.3 to 10 GHz. The overall impedance bandwidth of the antenna-AMC is 110% from 3.2 to 11 GHz. The peak gain of 7.2 dB is obtained at 5 GHz with compact dimensions of $40 \times 40 \times 6.5 \text{ mm}^3$. A gain improvement of 1.35 to 4.5 dB is observed for the entire UWB range with a unidirectional radiation pattern. The proposed antenna-AMC is fabricated and measured for verification. The designed antenna shows a wide bandwidth, good gain, high efficiency, and compact size.

REFERENCES

1. Saeidi, T., I. Ismail, W. P. Wen, A. R. Alhawari, and A. Mohammadi, "Ultra-wideband antennas for wireless communication applications," *International Journal of Antennas and Propagation*, Vol. 2019, Article ID 7918765, 2019.
2. Tahar, Z., X. Dérobert, and M. Benslama, "An ultra-wideband modified Vivaldi antenna applied to through the ground and wall imaging," *Progress In Electromagnetics Research C*, Vol. 86, 111–122, 2018.
3. Chen, Z. N., Y. Juan, X. Qing, and W. Che, "Enhanced radiation from a horizontal dipole closely placed above a PEC ground plane using a parasitic strip," *IEEE Transactions on Antennas and Propagation*, Vol. 64, No. 11, 4868–4871, 2016.
4. Kurra, L., M. P. Abegaonkar, A. Basu, and S. K. Koul, "FSS properties of a uniplanar EBG and its application in directivity enhancement of a microstrip antenna," *IEEE Antennas and Wireless Propagation Letters*, Vol. 15, 1606–1609, 2016.
5. Qin, P. Y., L. Y. Ji, S. L. Chen, and Y. J. Guo, "Dual-polarized wideband Fabry-Pérot antenna with quad-layer partially reflective surface," *IEEE Antennas and Wireless Propagation Letters*, Vol. 17, No. 4, 551–554, 2018.
6. Kundu, S., A. Chatterjee, S. K. Jana, and S. K. Parui, "A compact umbrella-shaped UWB antenna with gain augmentation using frequency selective surface," *Radioengineering*, Vol. 27, No. 2, 448–454, 2018.
7. Kumar, R. and D. C. Dhubkarya, "UWB compact microstrip patch antenna with high directivity using novel star-shaped frequency selective surface," *Progress In Electromagnetics Research C*, Vol. 119, 255–273, 2022.
8. Paik, H., S. K. Mishra, C. M. S. Kumar, and K. Premchand, "High performance CPW fed printed antenna with double layered frequency selective surface reflector for bandwidth and gain improvement," *Progress In Electromagnetics Research Letters*, Vol. 102, 47–55, 2022.
9. Zheng, Q.-R., B.-C. Lin, and B.-H. Zhou, "Design of high gain lens antenna by using 100% transmitting metamaterials," *Progress In Electromagnetics Research C*, Vol. 86, 167–176, 2018.
10. Manikandan, R., P. H. Rao and P. K. Jawahar, "Gain enhancement of horn antenna using metasurface lens," *Advanced Electromagnetics*, Vol. 7, No. 4, 27–33, 2018.

11. Pandit, V. K. and A. R. Harish, "Compact wide band directional antenna using cross-slot artificial magnetic conductor (CSAMC)," *International Journal of RF and Microwave Computer-Aided Engineering*, Vol. 29, No. 4, 21577, 2019.
12. Joshi, A. and R. Singhal, "Gain enhancement in probe-fed hexagonal ultra-wideband antenna using AMC reflector," *Journal of Electromagnetic Waves and Applications*, Vol. 33, No. 9, 1185–1196, 2019.
13. Mersani, A., L. Osman, and J.-M. Ribero, "Flexible UWB AMC antenna for early stage skin cancer identification," *Progress In Electromagnetics Research M*, Vol. 80, 71–81, 2019.
14. Jiang, Z., Z. Wang, L. Nie, X. Zhao, and S. Huang, "A low-profile ultrawideband slotted dipole antenna based on artificial magnetic conductor," *IEEE Antennas and Wireless Propagation Letters*, Vol. 21, No. 4, 671–675, 2022.
15. Gao, G. P., C. Yang, B. Hu, R.-F. Zhang, and S.-F. Wang, "A wearable PIFA with an all-textile metasurface for 5 GHz WBAN applications," *IEEE Antennas and Wireless Propagation Letters*, Vol. 18, No. 2, 288–292, Feb. 2019.
16. Zhu, J., S. Li, S. Liao, and Q. Xue, "Wideband low-profile highly isolated MIMO antenna with artificial magnetic conductor," *IEEE Antennas and Wireless Propagation Letters*, Vol. 17, No. 3, 458–462, Mar. 2018.
17. Abdulhasan, R. A., R. Alias, K. N. Ramli, F. C. Seman, and R. A. Abd-Alhameed, "High gain CPW-fed UWB planar monopole antenna-based compact uniplanar frequency selective surface for microwave imaging," *Int. J. RF Microw. Comput.-Aided Eng.*, Vol. 29, No. 8, Art. no. e21757, 2019.
18. Kumari, P., R. K. Gangwar, and R. K. Chaudhary, "An aperture-coupled stepped dielectric resonator UWB MIMO antenna with AMC," *IEEE Antennas and Wireless Propagation Letters*, Vol. 21, No. 10, 2040–2044, Oct. 2022.
19. Zhang, Y., Y. Li, W. Zhang, Z. Zhang, and Z. Feng, "Omnidirectional antenna diversity system for high-speed onboard communications," *Engineering*, Vol. 11, No. 4, 72–79, 2022.
20. Al-Gburi, A. J. A., I. B. M. Ibrahim, M. Y. Zeain, and Z. Zakaria, "Compact size and high gain of CPW-fed UWB strawberry artistic shaped printed monopole antennas using FSS single layer reflector," *IEEE Access*, Vol. 8, 92697–92707, 2020.
21. Joubert, J., J. C. Vardaxoglou, W. G. Whittow, and J. W. Odendaal, "CPW-fed cavity-backed slot radiator loaded with an AMC reflector," *IEEE Transactions on Antennas and Propagation*, Vol. 60, No. 2, 735–742, 2011.
22. Cao, Y. F., X. Y. Zhang, and T. Mo, "Low-profile conical-pattern slot antenna with wideband performance using artificial magnetic conductors," *IEEE Transactions on Antennas and Propagation*, Vol. 66, No. 5, 2210–2218, 2018.
23. Wu, J., B. Wang, W. S. Yezunis, and K. H. Teo, "Wireless power transfer with artificial magnetic conductors," *2013 IEEE Wireless Power Transfer (WPT)*, 155–158, IEEE, 2013.
24. Pandey, G. K., H. S. Singh, and M. K. Meshram, "Platform tolerant UWB antenna over multi-band AMC structure," *Microwave and Optical Technology Letters*, Vol. 58, No. 5, 1052–1059, 2016.
25. Sayidmarie, K. H. and L. S. Yahya, "Modeling of dual-band crescent-shape monopole antenna for WLAN applications," *International Journal of Electromagnetics and Applications*, Vol. 4, No. 2, 31–39, 2014.